Proceedings of SPIE, Vol. 5090, April 2003

Passive Detection of Buried Structures Using Elastic Waves

Pelham D. Norville and Waymond R. Scott, Jr.
School of Electrical and Computer Engineering
Georgia Institute of Technology
Atlanta, GA 30332-0250

ABSTRACT

An investigation of the feasibility of detecting structures buried underground through passive listening techniques will be presented. Passive detection of structures will be analyzed using elastic wave sources originating inside the structure and from sources exterior to the structure and on the surface. The primary method of investigation will be numerical models using the finite-difference time-domain method (FDTD).

A source inside the structure excites elastic waves in the structure, a portion of which travel upward along the walls of the structure and onward to the surface. An alternate form of excitation is a source such as a train, large vehicle, or an explosion located on the surface, away from the structure. Waves from this source interact with the structure and a portion of them travel up from the structure to the surface.

An array of sensors is constructed to map the field at the surface and to determine the location and basic characteristics of the structure. Generally, structures examined will be on the order of the size of an underground tunnel complex or buried room and elastic wave sources will be in the low frequency range of large machinery or vehicles.
Keywords: acoustic, seismic, passive, detection, buried structure

1. INTRODUCTION

The detection and localization of buried structures is a problem relevant to many different applications. Applications of interest include the detection of bunkers, hidden storage facilities, underground production facilities or factories, and covert smuggling tunnels. In each of these applications it can be assumed that noise sources inside the structures will produce elastic wave disturbances which will couple to the structure and be radiated to the surface.

The use of a passive detection scheme which monitors these signals has several advantages over an active detection scheme. One of the most important is that it allows the investigator's search to remain unknown to the occupants of the structure. A passive detection scheme also allows one to gather frequency response data regarding the elastic buried wave source. This data could be useful in determining the type of source (eg. a ventilation system, large generator, etc.)

In addition to monitoring signals emitted from a source inside the structure, known sources on the surface, such as a vehicle or large piece of machinery, may be used as a pre-existing active elastic wave source. The waves emitted from this source propagate down towards the structure, interact with it, and return to the surface in a characteristic pattern which allows for detection of the structure. A numerical model using the finite-difference time-domain (FDTD) technique will be constructed to study the interaction of elastic waves with the buried structure.

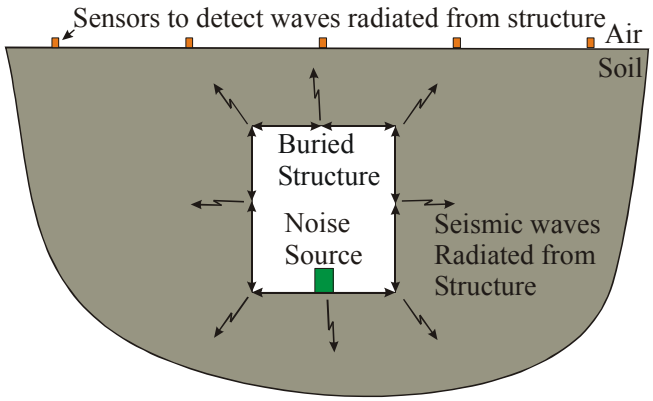

Figure 1: Illustration of buried structure detection scheme. A noise source in the structure radiates energy into the structure which propagates to the surface and is detected by a sensor array.

2. NUMERICAL MODEL

The numerical technique used to create the model is the three-dimensional finite-difference time-domain (FDTD) method. A first-order particle-velocity and mechanical-stress formation for the elastic wave fields is developed and then discretized from its continuous differential form. The solution space is then divided into a grid composed of individual cubes known as unit cells. Each of the elastic wave stresses and velocities are located at discrete spatial points in the three dimensional grid. Using the finite differences between field quantities in adjacent unit cells, the field quantities are computed at each discrete time step. The solution space is surrounded on all 4 sides and the bottom by a Perfectly Matched Layer (PML) which absorbs all outgoing waves. This prevents reflections from the edges of the grid, which makes the solution space appear as an infinite half-space. The top surface of the grid is terminated using a free surface boundary condition, which approximates the air-soil interface. A detailed description of the model can be found in the literature[1].

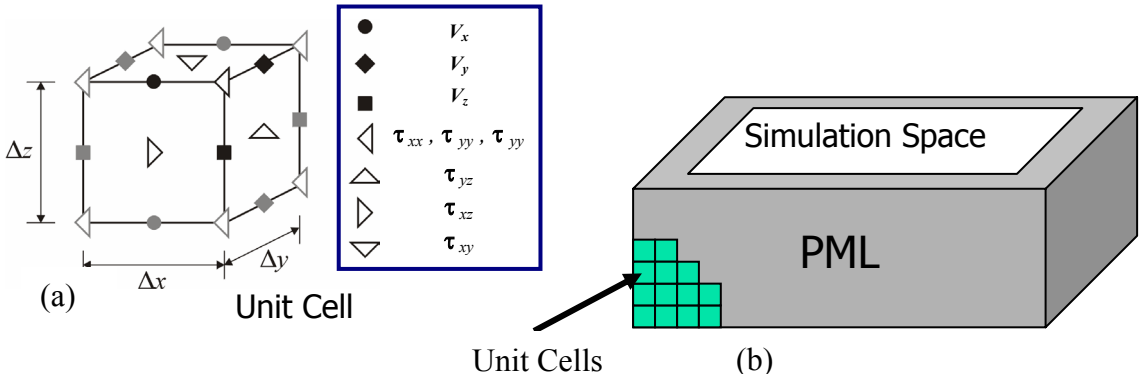

Figure 2: (a)The unit cell for the FDTD model. (b) The solution space for the FDTD simulation: composed of unit cells. The center is the area of the simulation while the edges are terminated by a perfectly matched layer (PML).

3. MODEL PARAMETERS

In order to ensure that the model will be representative of a physical case, the parameters used in the model must be an accurate depiction of the physical environment.

3.1. General FDTD Parameters

Several parameters are used to define the solution space for the model. The physical size of the solution space is approximately 32m x 8m x 7.5m of soil in which the structure was buried. Exploiting symmetry allows only one half of the solution space to be simulated. This space was discretized into equally sized unit cells of 0.07m on a side for a total size of 458 x 57 x 108 cells. The solution space was surrounded on four sides and the bottom with a 10 cell thick Perfectly Matched Layer (PML) to absorb outgoing waves. The surface was terminated in a free surface boundary to simulate the air-soil interface. The time step (Δt) between successive calculations was set at 10.5μs and the simulation was run for approximately 300ms for a total of 28383 time steps. The computation of results was performed on a 64 node Beowulf Cluster of Athlon XP 2200+ processors and required approximately 3 hours for computation of the results.

3.2. Buried Structure

Buried structures that would be of interest are generally very complicated in their design and layout. The structures of interest would in general be composed of multiple chambers and interconnecting tunnels. Since each structure will differ greatly from the next in its physical layout, it is simplest to simulate a single concrete walled room. The results obtained from the interaction with a simple structure can be used as a building block when trying to determine what to expect when analyzing a more complicated structure. The buried structure for these simulations is a single air chamber surrounded by 28cm thick concrete walls. The interior dimensions of the structure are approximately 2m x 3m x 3m .

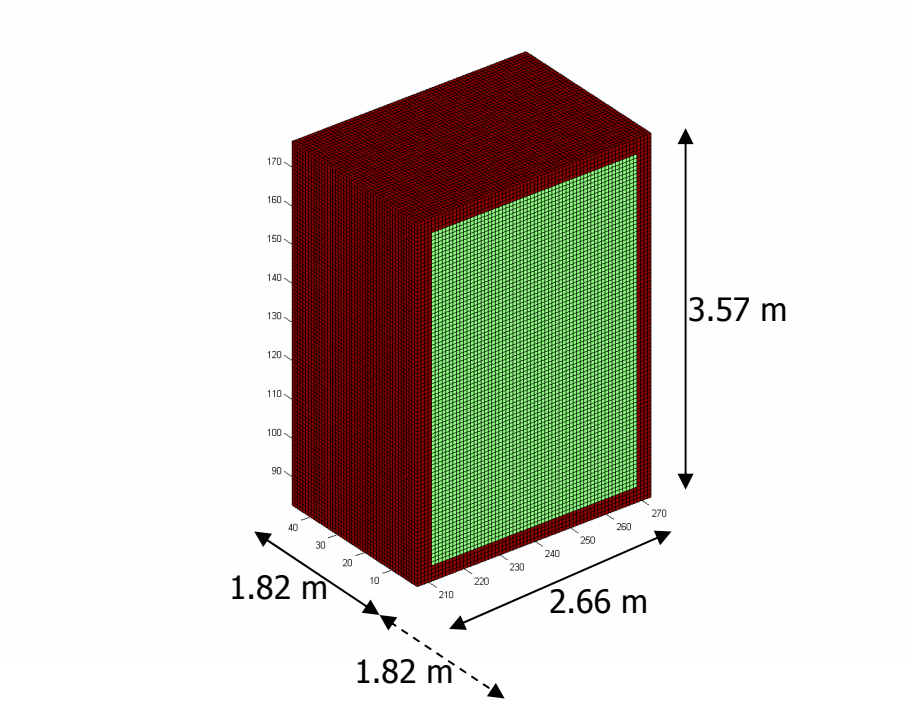

Figure 3: FDTD computational model for buried structure. The light colored interior is air. The dark colored walls are concrete. Only half the structure is shown so that the interior may be seen.

The material parameters of concrete can vary over a large range, so a median set of values was chosen that would be in the normal range for concrete used for the construction of buildings[2]. The structure itself is buried approximately 2.7m under the surface. The depth at which an actual structure would be buried could vary significantly depending on the application of the structure. This depth was chosen since it allows sufficient space between the surface of the soil and the top of the structure to eliminate any sort of resonance behavior that, for the frequencies of interest, would be uncharacteristic of a structure buried at depth. In addition, the depth of 2.7m allows for the waves that interact with the structure to spread out sufficiently to discern the pattern that will arrive at the surface.

3.3. Soil Parameters

In general, the soil is composed of multiple layers, each with its own set of characteristics. To accurately model a buried structure, it is necessary to have a good understanding of the soil in which the structure would be buried. The soil types in which structures could be buried can vary greatly between locations. In order to create an accurate model, a specific soil profile was chosen to use for all the models. This soil profile was generated from a soil survey performed at an arid government test facility[3]. The profile provided is a soil survey completed over a 200.5 m x 75.5 m area to a depth of 26.5 m. The resolution of the profile is 50cm in each direction. From this 3-D profile, the soil parameters were averaged at each depth to give a 1-D soil profile that varies with depth. The layers used in the model are 49cm thick, which is very close to the 50cm layers that the averaged depth profile created. Therefore, soil properties were not averaged for layers in the model which extended slightly into an adjacent layer in the soil survey data.

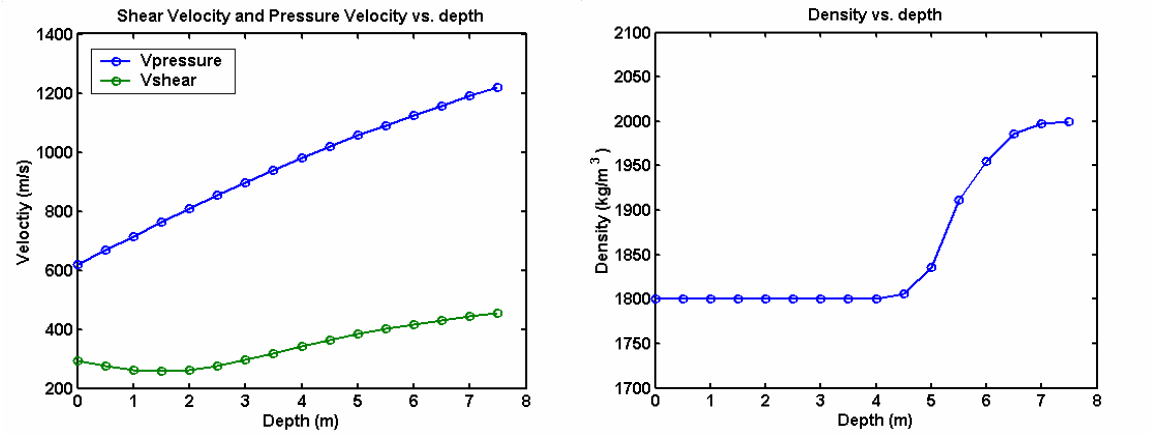

Figure 4: Averaged Soil Parameters for model based on soil survey results.

3.4. Elastic Wave Source

The source used in the numerical model is a differentiated gaussian pulse point source with a center frequency of 60 Hz. The differentiated gaussian pulse was chosen since it can be used to see the effects from a range of frequencies centered around 60Hz. The justification for the choice of 60Hz as a center frequency is that most large pieces of machinery and vehicles would serve as elastic wave sources in this frequency range.

The quantity excited by the numerical source is the particle velocity in the vertical direction. Here, the vertical particle velocity is set to be equal to the value of the excitation pulse at the location of the source.

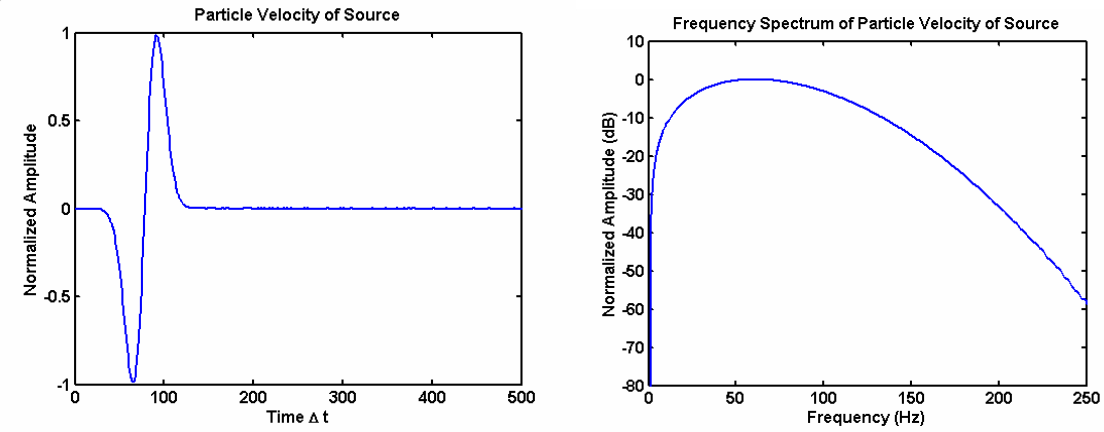

Figure 5: Differentiated Gaussian Source Signal Characteristics

4. RESULTS

Using the numerical model, the results of two cases will be presented. First, a source will be located on the interior surface of the "floor" of the buried structure. Next, a case will be presented of a source on the surface and approximately 14m away from the structure.

4.1. Source Inside Structure

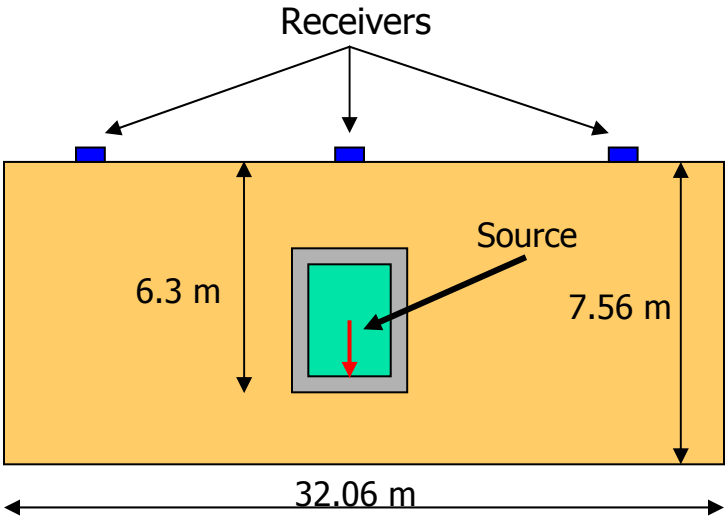

Figure 6: Layout of Case 1: Source located inside the structure

For the first case (Fig. 6), the source is placed on the floor of the buried structure and excites waves that couple both into the air in the room and into the concrete walls on the structure. In Figs. 7 and 8, pseudo color graphs of the magnitude of the vertical component of the particle velocity are presented for three instants in time. The pseudo color scale is a 60 dB logarithmic scale from white (0 dB) to black (-60 dB). The graphs in Fig. 7 are for an xy plane cut through the center of the structure. The graphs in Fig. 8 are for an xz plane cut along the air-soil interface at the surface. The source generates a disturbance that couples into the walls of the structure and travels quickly through the concrete to reach the top surface of the structure.

The structure radiates pressure, shear and Rayleigh waves. The shear and Rayleigh waves are labeled in Fig. 7.3; the pressure wave, being a faster moving wave, has already propagated outside the computational domain. The walls guide the waves to the top of the structure where these waves produce a characteristic pattern on the surface with an obvious center [Fig 8]. From the location of this pattern, it is possible to determine the location on the surface which is directly above the structure. However, this set of data provides little information about the depth at which the structure is buried.

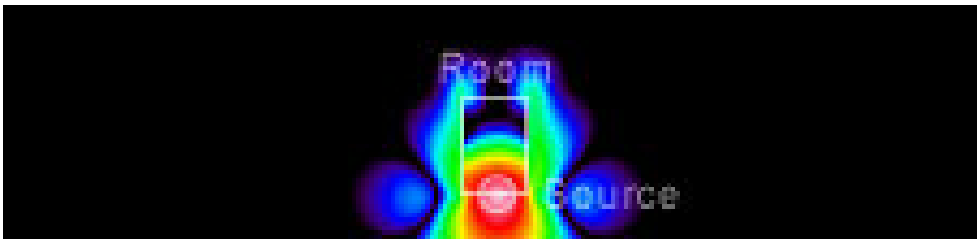

Figure 7.1: Time Index: 13.66ms. *yz* plane cut. Waves are guided along concrete walls of structure

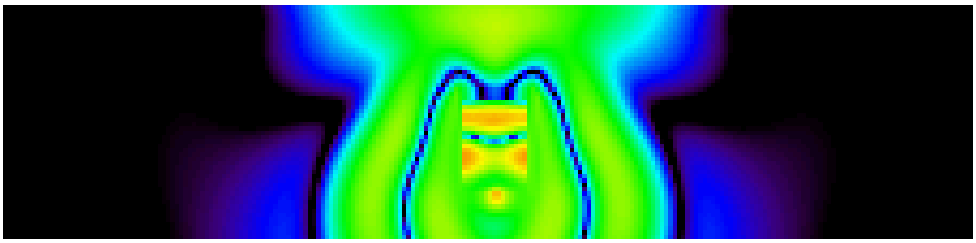

Figure 7.2: Time Index: 22.49ms. *yz* plane cut. Waves radiate off top of structure and arrive at surface

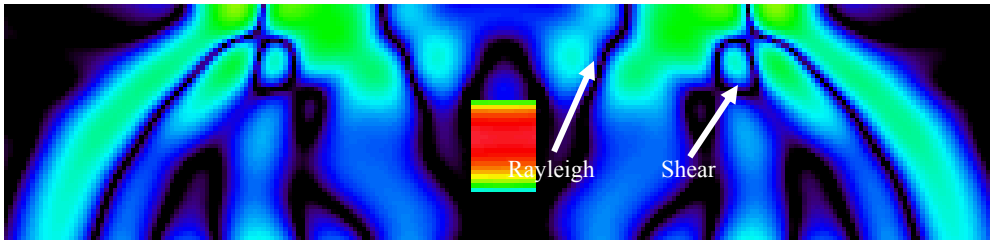

Figure 7.3: Time Index: 45.79ms. *yz* plane cut.
Shear and Rayleigh waves propagate away from the structure

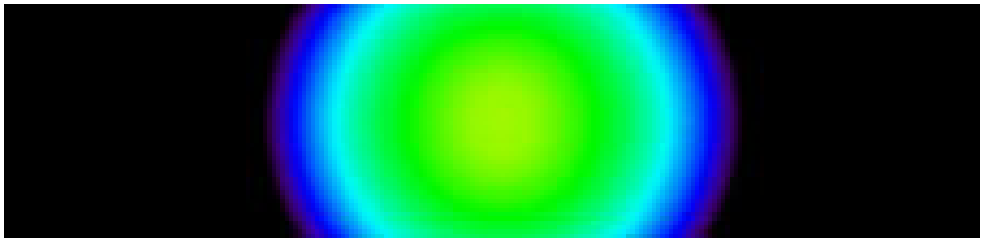
Figure 8.1: Time Index: 22.49ms. *xy* plane cut. Waves arrive at surface in characteristic pattern

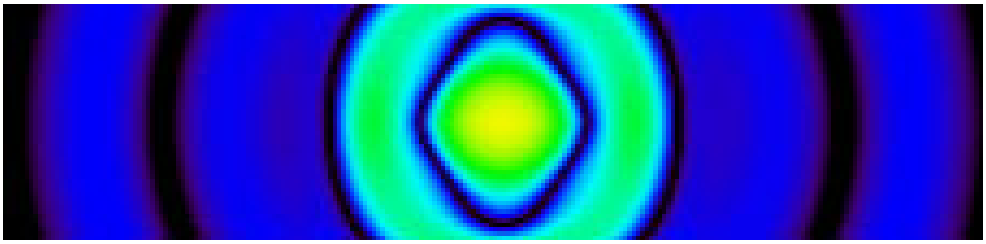
Figure 8.2: Time Index: 32.133ms. *xy* plane cut. Even in late time, a characteristic pattern is discernable.

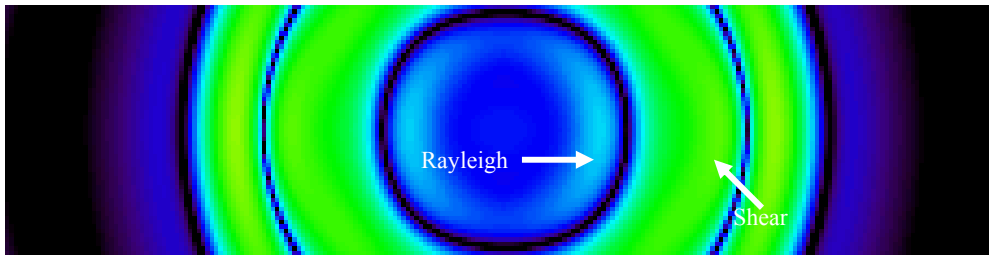

Figure 8.3: Time Index: 67.48ms. *xy* plane cut. Rayleigh and Shear waves propagate away from structure.

Note that while the particle velocity inside the room remains high for late time, the energy inside the room is very low, but it is trapped due to the large impedance difference between the concrete walls and the air in the chamber. This explains why even in Fig. 7.3, the room is still visible after the waves have moved away from the structure.

The second type of plot presented is a waterfall graph (Fig. 9). Each line is a trace of vertical particle velocity vs. time at a point. Traces are recorded for a number of points along a line on the surface. These traces are offset along the vertical axis by the distance from the source at which they are recorded. The result is a graph which shows the propagation of waves along the surface of the solution space. The waves propagate away from the point on the surface directly above the center at various speeds. The fastest waves have steeper slopes ($\Delta x / \Delta t$). From this plot, it can also be seen that the waves propagate symmetrically away from a point on the surface directly above the center of the structure, indicating a symmetric structure beneath the surface from which the waves have originated.

From the waterfall graph, the different waves can be identified based on the speed at which they propagate across the surface. The three primary waves which are identified are the Rayleigh wave, the shear wave, and the pressure wave (Fig. 9). These waves can also be seen in the pseudo color images (Fig. 7,8), but the waterfall graph data is useful for determining the wave speeds. The slope of a line traced through the disturbance caused by each wave represents the wave speed. The wave speeds determined from the graph in this case are: $V_{Rayleigh} \approx 290$ m/s, $V_{Shear} \approx 460$ m/s, $V_{Pressure} \approx 960$ m/s. These are roughly the wave speeds that would be anticipated, given the velocity profiles in Fig. 4. It is possible to more accurately determine the soil characteristics from surface data collected from the propagating waves[4,5]. These methods are more accurate than the approximation used in this paper, but are also significantly more complicated.

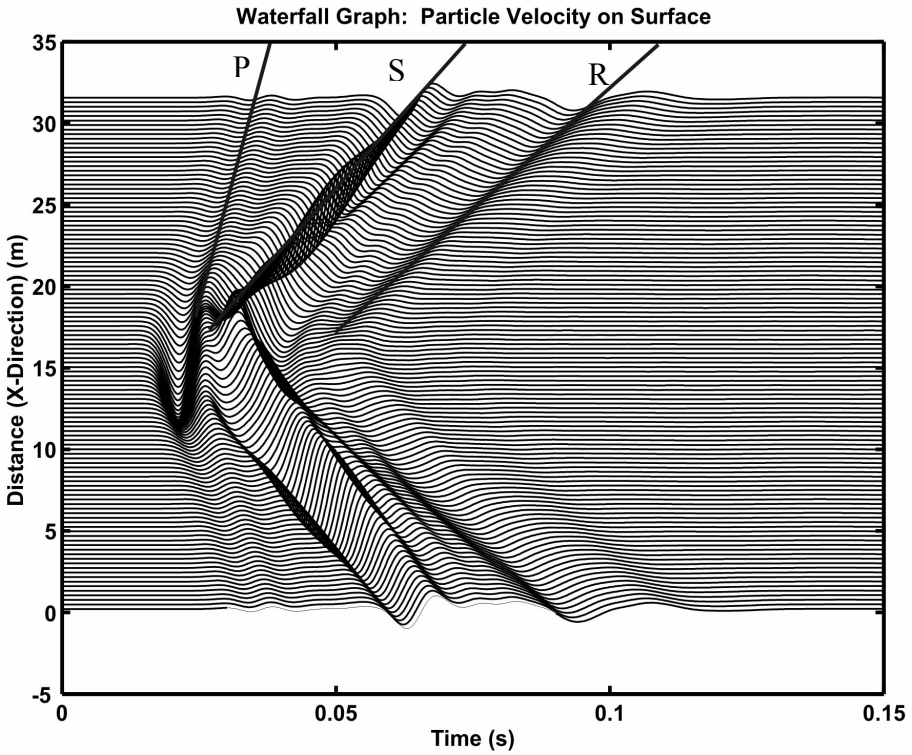

Figure 9: Waterfall graph of vertical particle velocity on the surface. Note that waves arrive first at the center of the space, directly above where the structure is located. Rayleigh (R), Shear (S), and Pressure (P) waves are identified by the speed at which they propagate and noted on figure.

Because of the characteristic pattern given off by the source located in the buried structure, it is simple to determine the location of the source in the *xy* plane on the surface using either waterfall data or the pseudo color plot. Using the waterfall data, it may be possible to determine the approximate depth of the source. This may be done by noting the difference in time between when any two of the wave types arrive at the surface at a given point.

If it is assumed that the source of the waves is a simple point source buried in homogeneous soil, then it becomes possible to estimate the depth at which the source is buried. In order to apply this simple approximation to the results which have been presented in this paper, the wave speeds are assumed to be those that were determined from the waterfall graph in Fig. 9. The point directly above the source is selected, and the time delay between the arrival of the pressure and shear waves at this point is found to be and $\Delta t = 0.01$s. Solving for depth,

$$D \approx \frac{\Delta t}{\frac{1}{V_{Shear}} - \frac{1}{V_{\Pr essure}}} = 8.85m$$

which is in comparison to the known depth of the source of 6.3m. This estimate is surprisingly accurate, given that the source is not actually buried in soil, but contained in the structure. The walls of the structure will cause the waves to propagate at different speeds. This is because the different wave types will couple into the structure differently, thereby decreasing the accuracy of the measurement.

The waterfall and pseudo color graphs provide a view of the data that could be gathered using a large number of sensors. The multiple wave types present in this data are easily identified when a large number of spatial points are measured. While this provides a great deal of information which allows for the source location to be identified, this number of sensors may be impractical in an experimental set up. Through continued modeling, the propagation characteristics of each of these waves can be further defined, such that ultimately, data may be taken at only a few discrete points to determine the location from which all the waves propagate, and to separate the waves. Time domain and frequency response data from a few representative points are presented below as an example of this approach.

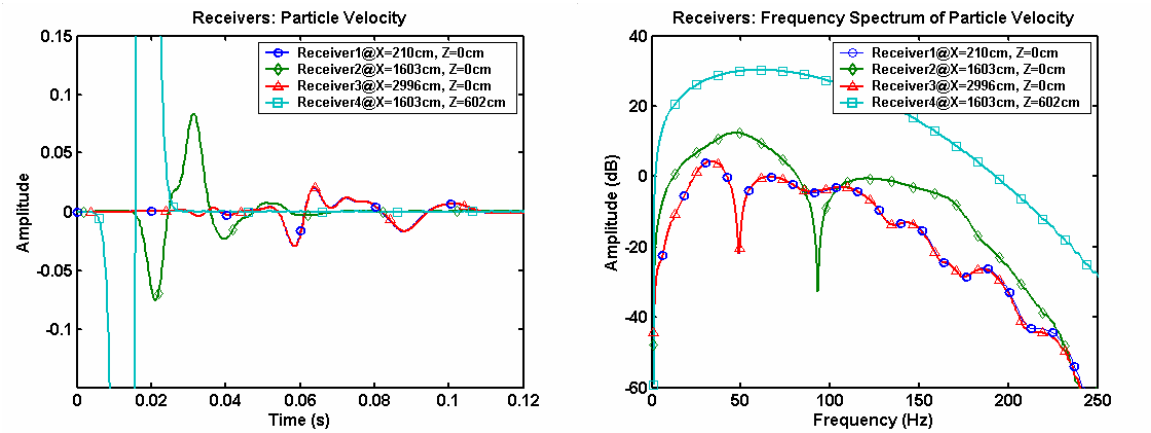

Figure 10: Vertical Particle Velocity measured at the source and 3 additional locations. Time domain and Frequency Response data are presented.

4.2. Source on the Surface

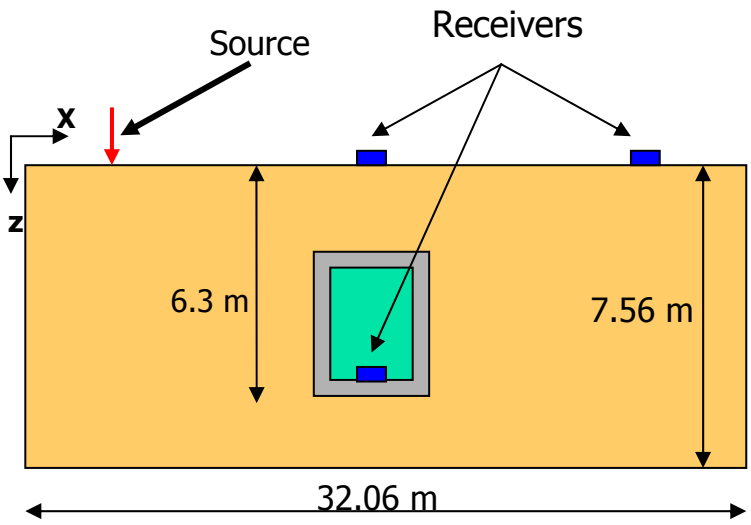

Figure 11: Layout of Case 2: Source located on the surface

In the second case (Fig. 11), the source is located on the surface approximately 14m away from the structure. This source approximates a large vehicle or surface machine which creates seismic waves that are coupled into the ground which would then propagate towards the structure. In this case, the pattern produced at the surface by the waves reflected from the structure will not be symmetrical. Instead, the primary method of detection is by the change in the behavior of the Rayleigh wave front that travels away from the source. Since the characteristics of the shear and Rayleigh waves at the surface are dependent on the subsurface topology, there is a disturbance that occurs when waves reflected from the left side of the structure arrive at the surface and disturb the rightward propagating surface wave.

Figs. 12 and 13 show the waves propagating away from the source, located on the surface to the left of the structure. The wave fronts have just arrived at the structure such that on the surface, no difference is yet apparent between the case with the structure (Fig. 12) and the one without the structure (Fig. 13). The Rayleigh and shear waves have been labeled in Fig. 12.

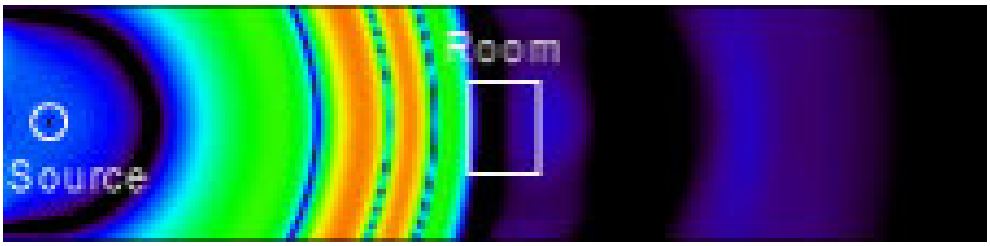

Figure 12.1: *xz* plane cut

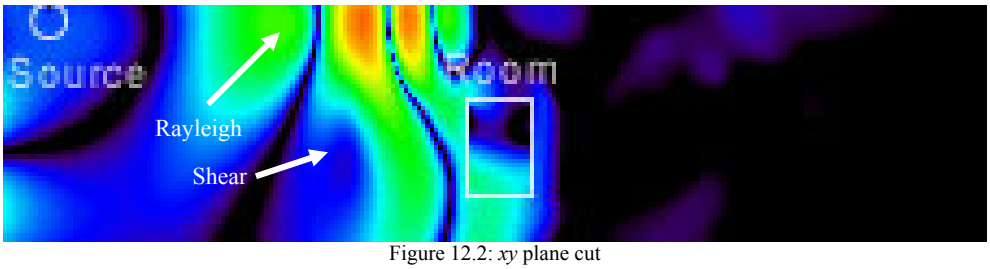

Figure 12.2: *xy* plane cut

Figure 12: Time Index: 59.45ms. Structure present. Waves arrive at left edge of structure.

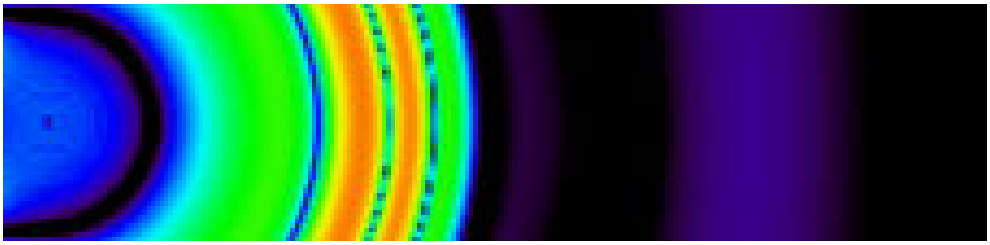

Figure 13.1: *xz* plane cut

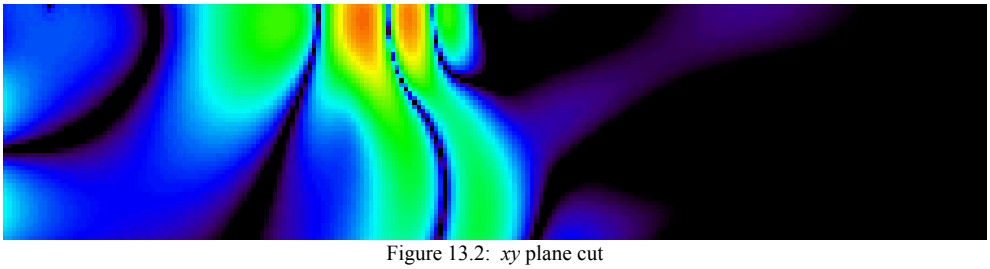

Figure 13.2: *xy* plane cut

Figure 13: Time Index: 59.45ms. Structure absent. No change yet from case with structure present.

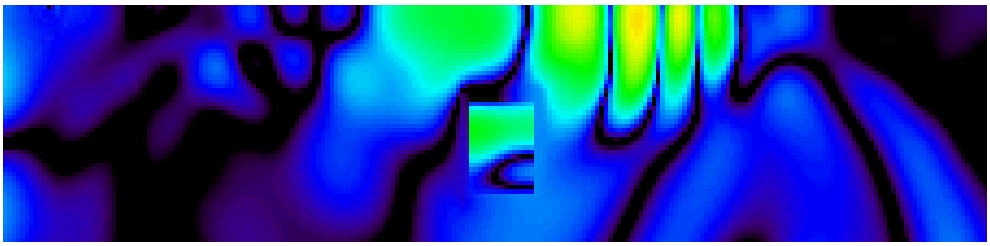

Figure 14.1: *xy* plane cut

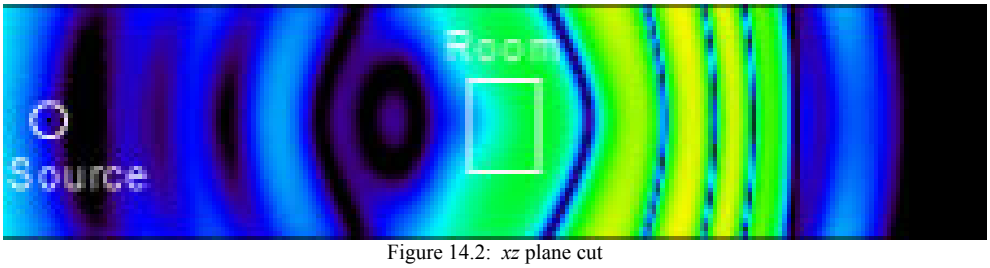

Figure 14.2: *xz* plane cut

Figure 14: Time Index: 93.19ms. Structure present. Surface waves pass over top of structure. Reflections can be seen on the surface to the left of the structure.

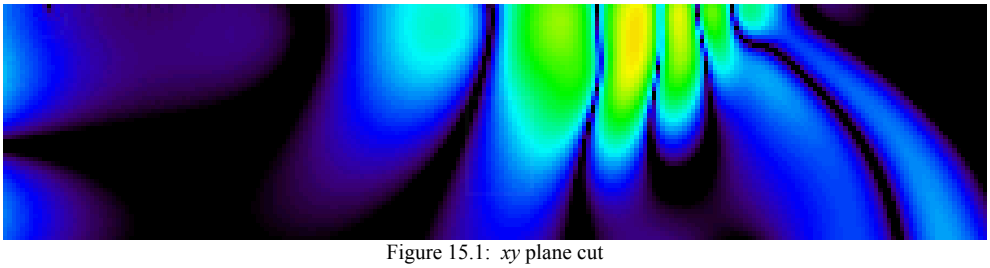

Figure 15.1: *xy* plane cut

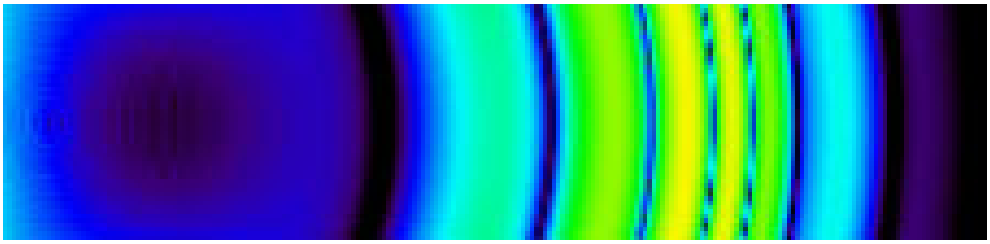

Figure 15.2: *xz* plane cut

Figure 15: Time Index: 93.19ms. Structure absent. Surface waves propagate undisturbed. No reflections are noted on the surface.

In Fig. 14, the disturbance from the reflected waves is apparent when compared to Fig. 15. It can be seen that when the wave arrives at the structure, traveling from the surface, very little energy is coupled into the structure. Most of the waves are reflected off the left side of the structure, or they are guided up the sides of the structure to the surface to produce the disturbance to the left of the structure.

It should also be noted that because the behavior of surface waves is dependent the materials parameters of the soil within 1 or 2 wavelengths of the surface, only lower frequency components of the surface waves will extend deep enough to interact with the structure. Therefore, the deeper the structure is buried, the less visible it will be for a higher frequency source. This will become more apparent after examining the wave velocities in the waterfall graphs.

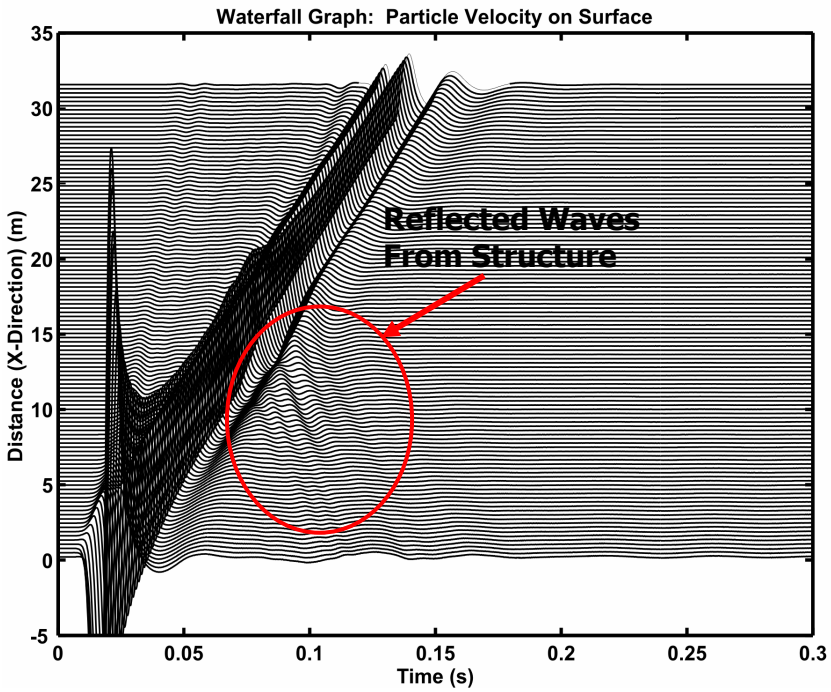

Figure 16: Waterfall graph of the vertical particle velocity on the surface. The large pulse near t = 0, x = 0 is from the source. The waves reflected off the structure have been identified.

In Fig. 16, the source is located at the left edge of the solution space. The large pulse that occurs near t = 0, and x = 0 is the source excitation. In this mode, because the excitation is on the surface, the majority of the energy is radiated in the forward traveling Rayleigh wave[6], which dominates the response, as can be seen in Fig. 16. The waterfall graphs presented for this case show the waves reflected from the structure as lines with negative slope. The second waterfall, Fig. 17, has the amplitude clipped since the source causes saturation at a level far below the optimal level for viewing the reflections from the structure.

The reflected waves from the structure are indicated on the waterfall plot, and identified as the shear and Rayleigh waves. The velocities of these waves were determined to be: $V_{shear} \approx 581.8$ m/s and $V_{Rayleigh} \approx 333.3$ m/s. These velocities are slightly higher than the ones calculated in the case for the source in the structure. The differences can be attributed to the fact that the structure interacts differently with waves that originate on the surface. The depth to which surface waves penetrate is dependent on wavelength. Because the structure is buried a significant distance under the surface, only the low frequency components are reflected off the structure. These low frequency components have a higher phase velocity than the center frequency of the excitation pulse. In the case with the source in the structure, the center frequency dominates the response, which causes the measured wave velocity to be higher. These wave speed discrepancies confirm that only the low frequency components are interacting with the structure. Therefore the deeper the structure is buried, the lower the frequencies that are needed to detect it using a surface source.

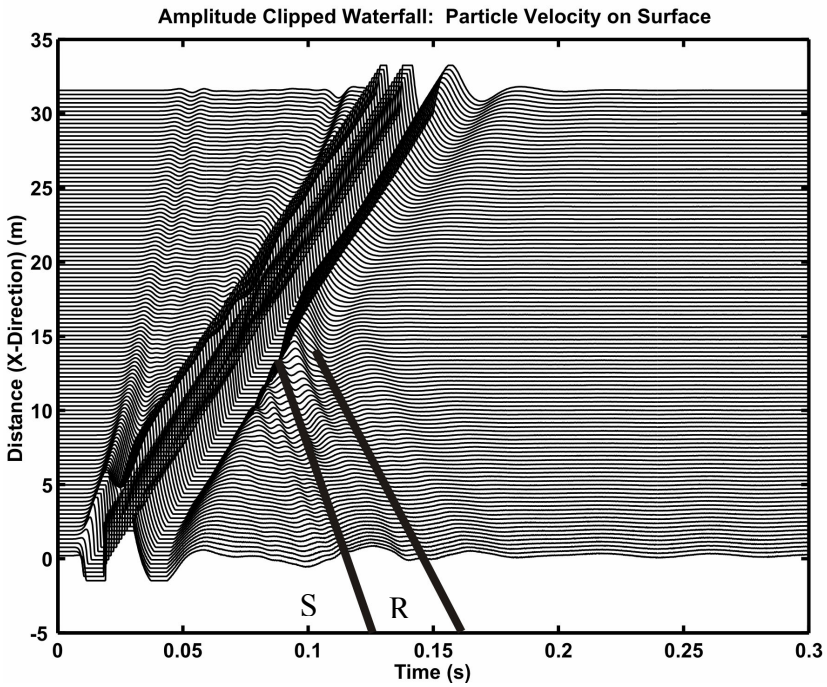

Figure 17: The same plot as Fig. 16, but with the amplitude clipped to remove the source. This allows for greater resolution of the reflected waves.

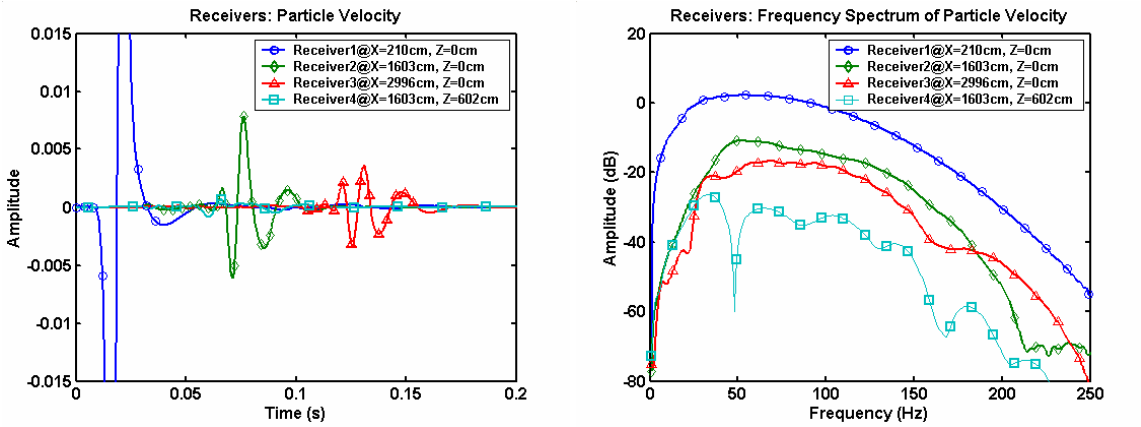

Figure 18: Vertical particle velocity measured at the source and 3 additional locations. Time domain and frequency response data are presented.

As with the case of the source inside the structure, gathering data at many spatial locations allows for easier detection of the buried structure. As can be seen from the data gathered at points on the surface, the reflected waves are not readily visible if the points at which data are taken are not within the area of the disturbance that lies just to the left of the structure. In this case, more sensors are required in order to locate the structure.

5. CONCLUSIONS

It is possible to locate a buried structure using the passive detection of elastic waves. The detection probability and the anticipated results of the pattern radiated from or reflected off of the buried structure are strongly dependent on the soil characteristics, the depth at which the structure is buried, and the dimensions of the structure in proportion to the

wavelength of waves generated by the source. In general, a large number of surface sensors are necessary to accurately localize the source. Through further characterization of the response from different structure types, localization may become possible with a decreasing number of sensors on the surface.

ACKNOWLEDGEMENTS

This work is supported in part by the U.S. Army Research Office under contract number DAAD19-02-1-0252.

REFERENCES

1. C.T. Schröder,"On the Interaction of Elastic Waves with Buried Land Mines: an Investigation Using the Finite-Difference Time Domain Method" Doctoral Thesis, Georgia Inst. Of Technology, Atlanta, GA 2001.]

2. A. M. Neville, *Properties of Concrete, 3rd Ed.* Pitmann Publishing: London, 1981.

3. Miller, R.D., T.S. Anderson, J.C. Davis, D.W. Steeples, and M.L. Moran, 2001, 3-D characterization of seismic properties at the Smart Weapons Test Range, YPG: Proceedings of the 2001 meeting of the Military Sensing Symposia (MSS) specialty group on Battlefield Acoustic and Seismic Sensing, Magnetic and Electric Field Sensors, Laurel, MD, October 23, 2001. Published on CD.

4. G. D. Larson, J.S. Martin, W.R. Scott, Jr., J.H. McClellan, B. Declety, and P. D. Norville, "Surface-wave-based inversions of shallow seismic structure," *Proc. SPIE, 2003, AeroSense 21 – 25 April, 2003., Paper 5089-137.*

5. J. Carlos Santamarina, and Dante Fratta. *Introduction to Discrete Signals and Inverse Problems in Civil Engineering.* ASCE Press: Reston, Virginia, 1998.

6. K. F. Graff, *Wave Motion in Elastic Solids*, Clarendon Press, Oxford, 1975.